

Crystal Structure and Magnetic Properties of an Ionic C₆₀ Complex with Decamethylcobaltocene: (Cp*₂Co)₂C₆₀(C₆H₄Cl₂, C₆H₅CN)₂. Singlet–Triplet Transitions in the C₆₀²⁻ Anion

Dmitri V. Konarev,^{*†‡} Salavat S. Khasanov,[§] Gunzi Saito,^{*†} Ivan I. Vorontsov,^{||} Akihiro Otsuka,^{†,⊥} Rimma N. Lyubovskaya,[‡] and Yury M. Antipin^{||}

Division of Chemistry, Graduate School of Science, Kyoto University, Sakyo-ku, Kyoto 606-8502, Japan, Institute of Problems of Chemical Physics RAS, Chernogolovka, Moscow Region 142432, Russia, Institute of Solid-State Physics RAS, Chernogolovka 142432, Russia, Institute of Organoelement Compounds RAS, 28 Vavilov St., 117334 Moscow, Russia, and Research Center for Low Temperature and Materials Sciences, Kyoto University, Sakyo-ku, Kyoto 606-8502, Japan

Received January 5, 2003

The C₆₀ complex with decamethylcobaltocene, (Cp*₂Co)₂C₆₀(C₆H₄Cl₂, C₆H₅CN)₂ (**1**) (C₆H₄Cl₂ = 1,2-dichlorobenzene; C₆H₅CN = benzonitrile), has been obtained as single crystals by the diffusion method. The IR and UV–vis–NIR spectra show the presence of the C₆₀²⁻ and the Cp*₂Co⁺ ions, which form a three-dimensional framework with channels accommodating solvent molecules. EPR and SQUID measurements show that C₆₀²⁻ has a diamagnetic singlet (*S* = 0) state in the 2–140 K range. The appearance of a broad EPR signal and the increase in magnetic susceptibility of **1** above 140 K are assigned to a thermal population of a close lying triplet (*S* = 1) state. The singlet–triplet energy gap for C₆₀²⁻ in solid **1** is estimated to be 730 ± 10 cm⁻¹.

Ionic compounds of fullerenes show interesting physical¹ and structural² properties. Fullerenes have unique electronic structure with a 3-fold degenerate LUMO (t_{1u}), which is able to accept up to 6 electrons to form anions from -1 to -6.³ Up to now, crystal structures of several C₆₀²⁻ salts were solved: PPN₂C₆₀ (PPN⁺ = bis(triphenylphosphine)iminium),⁴ [M(NH₃)₆] C₆₀(NH₃)₃ (M = Ni, Mn, and Cd),⁵ and [K(2,2,2-cryptand)]₂ C₆₀·(C₇H₈)₄ (C₇H₈ = toluene).⁶ Several polycrystalline compounds of C₆₀²⁻ are also known,³ including a solvent-free complex with decamethylcobaltocene: (Cp*₂Co)₂C₆₀.⁷ Despite this, the electronic structure of the C₆₀²⁻ dianion is still under discussion. Molecular orbital calculations show that C₆₀²⁻ can have a singlet ground state

with a triplet excited state and the energy gap of 300–1500 cm⁻¹.⁸ EPR study of C₆₀²⁻ in dimethyl sulfoxide (DMSO) shows a diamagnetic singlet (*S* = 0) ground state for this anion with a thermally populated excited triplet (*S* = 1) state and the energy gap of 600 ± 100 cm⁻¹.⁹ Recently, it has been found that (PPN⁺)₂(C₆₀²⁻) in DMSO is EPR silent in the 125–280 K range.¹⁰ Magnetic susceptibility measurements of solid (PPN⁺)₂C₆₀²⁻ also support a singlet ground state for C₆₀²⁻, however, with the nearly degenerate excited triplet state and the singlet–triplet energy gap of ~1 cm⁻¹.⁷ The effective magnetic moment of the C₆₀²⁻ salts, PPN₂C₆₀⁷ and [K(2,2,2-cryptand)]₂C₆₀·(DMF)₃ (DMF = *N,N*-dimethylformamide),⁶ was measured to be far from zero even at 4 K. In both salts, the temperature-dependent data do not allow the estimation of the singlet–triplet energy gap for the C₆₀²⁻ anion in the solid state.

In this work, we report the synthesis, crystal structure, and magnetic properties of the ionic C₆₀ complex with decamethylcobaltocene: (Cp*₂Co)₂C₆₀·(C₆H₄Cl₂, C₆H₅CN)₂ (**1**) (C₆H₄Cl₂ = 1,2-dichlorobenzene; C₆H₅CN = benzonitrile).

The crystals of **1** were prepared in anaerobic conditions by diffusion of *n*-hexane into the C₆H₄Cl₂/C₆H₅CN (50:50) solution containing C₆₀ and 2.4 molar equiv of Cp*₂Co. The composition of the complex was determined from the X-ray analysis.

The IR spectrum of **1** indicates the ionic ground state. The bands ascribed to C₆₀ appear at 1369s, 1182w, 574s, and 520w cm⁻¹. The F_{1u}(4) mode of C₆₀ (at 1429 cm⁻¹ in the

* Authors to whom correspondence should be addressed. E-mail: konarev@icp.ac.ru (D.V.K.); saito@kuchem.kyoto-u.ac.jp (G.S.).

† Division of Chemistry, Graduate School of Science, Kyoto University.

‡ Institute of Problems of Chemical Physics RAS.

§ Institute of Solid-State Physics RAS.

|| Institute of Organoelement Compounds RAS.

⊥ Research Center for Low Temperature and Materials Sciences, Kyoto University.

- (1) (a) Rosseinsky, M. J. *J. Mater. Chem.* **1995**, *5*, 1497. (b) Konarev, D. V.; Lyubovskaya, R. N. *Russ. Chem. Rev.* **1999**, *68*, 19.
- (2) (a) Prassides, K. In *The Physics of fullerene-based and fullerene-related materials*; Andreoni, W., Ed.; Kluwer Academic Publishers: Dordrecht, The Netherlands, 2000; p 175. (b) Konarev, D. V.; Khasanov, S. S.; Otsuka, A.; Saito, G. *J. Am. Chem. Soc.* **2002**, *124*, 8520.
- (3) Reed, C. A.; Bolskar, R. D. *Chem. Rev.* **2000**, *100*, 1075.
- (4) Paul, P.; Xie, Z.; Bau, R.; Boyd, P. D. W.; Reed, C. A. *J. Am. Chem. Soc.* **1994**, *116*, 4145.

- (5) (a) Himmel, K.; Jansen, M. *Eur. J. Inorg. Chem.* **1998**, 1183. (b) Himmel, K.; Jansen, M. *Chem. Commun.* **1998**, 1205.
- (6) Fässler, T. F.; Spiekermann, A.; Spahr, M. E.; Nesper, R. *Angew. Chem., Int. Ed. Engl.* **1997**, *36*, 486.
- (7) Boyd, P. D. W.; Bhyrappa, P.; Paul, P.; Stinchcombe, J.; Bolskar, R. D.; Sun, Y.; Reed, C. A. *J. Am. Chem. Soc.* **1995**, *117*, 2907.
- (8) (a) Negri, F.; Orlandi, G.; Zerbetto, F. *J. Am. Chem. Soc.* **1992**, *114*, 2909. (b) Yamaguchi, K.; Hayashi, S.; Okumura, M.; Nakano, M.; Mori, W. *Chem. Phys. Lett.* **1994**, *226*, 372.
- (9) Trulove, P. C.; Carlin, R. T.; Eaton, G. R.; Eaton, S. S. *J. Am. Chem. Soc.* **1995**, *117*, 6265.
- (10) Paul, P.; Kim, K.-C.; Sun, D.; Boyd, P. D. W.; Reed, C. A. *J. Am. Chem. Soc.* **2002**, *124*, 4394.

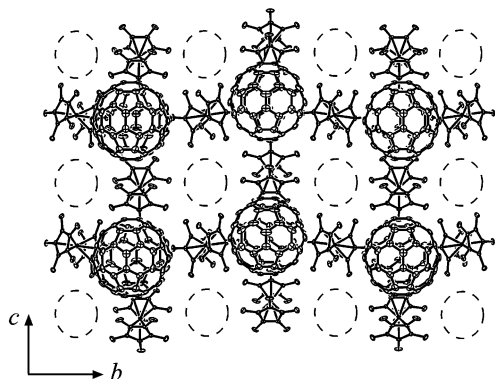


Figure 1. Projection of the crystal structure of **1** on the *bc*-plane. Dashed ellipses show the channels accommodating solvent molecules. Only the major orientation of C_{60}^{2-} is shown.

parent fullerene) is the most sensitive to charge transfer to the fullerene molecule.¹¹ This mode has an intermediate position (1369 cm^{-1}) between those for -1 and -3 charged C_{60} (1392 and 1363 cm^{-1} , respectively¹¹), indicating approximately -2 charge on the C_{60} molecules. The bands at 445m , 1020m , 1074w , 1369s (coincides with the $F_{1u}(4)$ mode of C_{60}), 1421w , 1436w , and $1473\text{w}\text{ cm}^{-1}$ are attributed to Cp^*_2Co .¹² The band of neutral Cp^*_2Co (429 cm^{-1}) shifts to 448 cm^{-1} in ionic $(Cp^*_2Co^+) \cdot (PF_6^-)$.¹¹ The position of this band at 445 cm^{-1} in **1** shows the formation of $Cp^*_2Co^+$.

The -2 charged state of C_{60} is confirmed by the UV–vis–NIR spectrum of **1** in the KBr matrix. The bands at 854 , 963 , and 1350 nm are characteristic of C_{60}^{2-} .^{3,13} The formation of a dianionic complex between Cp^*_2Co and C_{60} is possible due to $E^{+0}_{1/2}$ of Cp^*_2Co (-1.47 V^{12}) being essentially more negative than $E^{1-/2-}_{1/2}$ of C_{60} (-0.87 V^{14}).

The $Cp^*_2Co^+$ cations are ordered in the crystal structure of **1**,¹⁵ whereas the C_{60}^{2-} anions are fixed in two crystallographically independent orientations and the occupancy factors at a 4:1 ratio. Orientationally ordered $C_6H_4Cl_2$ and C_6H_5CN share the same crystallographic position with the occupancy factors at a 1:1 ratio.

Crystal packing of **1** can be described as a three-dimensional framework built of the alternating $Cp^*_2Co^+$ and C_{60}^{2-} ions with the channels accommodating solvent molecules (Figure 1). The similar channels were found in the hexagonal framework built of the $Cp^*_2Cr^+$ and $(C_{60}^-)_2$ dimers in ionic $Cp^*_2Cr \cdot C_{60} \cdot (C_6H_4Cl_2)_2$.^{2b} Each C_{60}^{2-} is surrounded by eight bulky $Cp^*_2Co^+$ cations. The shortest center-to-center distances between adjacent C_{60}^{2-} species are 12.10 , 12.57 , and 12.42 \AA along the *a*-, *b*-, and *c*-axes, respectively.

Among the eight $Cp^*_2Co^+$ cations surrounding C_{60}^{2-} , only four of them form shortened van der Waals contacts with

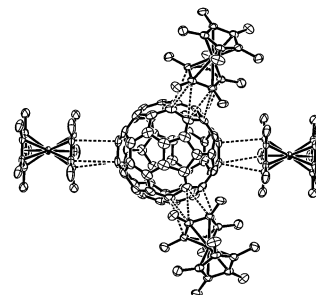


Figure 2. Van der Waals contacts ($<3.5\text{ \AA}$) between the $Cp^*_2Co^+$ and C_{60}^{2-} ions (dashed lines). Only the major orientation of C_{60}^{2-} is shown.

C_{60}^{2-} in the 3.07 – 3.50 \AA range (Figure 2). Numerous H ($Cp^*_2Co^+$) \cdots C(C_{60}^{2-}) contacts in the 2.9 – 3.1 \AA range additionally stabilize this crystal structure. Four $Cp^*_2Co^+$ species forming shortened van der Waals contacts with C_{60}^{2-} are distributed asymmetrically over its surface; three cations are located above one C_{60}^{2-} hemisphere, and only one cation is located above another hemisphere (Figure 2).

The mean values of the 6–6 and 6–5 bonds in C_{60}^{2-} were refined as free variable parameters and found to be $1.388(9)$ and $1.443(6)\text{ \AA}$, respectively. These bond lengths are close to those in $Cp^*_2Ni \cdot C_{60} \cdot CS_2$, $1.389(3)$ and $1.449(3)\text{ \AA}$,¹⁶ respectively, and PPN_2C_{60} , $1.399(2)$ and $1.446(2)\text{ \AA}$,⁴ respectively. The diameter of the C_{60}^{2-} anion in three orthogonal directions running through the oppositely located carbon atoms is equal to 7.077 , 7.086 , and 7.020 \AA . Thus, the ellipsoidal deviation is $\sim 0.06\text{ \AA}$. This value is more than two times larger than that for the parent C_{60} (0.025 \AA),¹⁷ approximately 1.5 times smaller than that in $Cp^*_2Ni \cdot C_{60} \cdot CS_2$ ($0.098(6)\text{ \AA}$)¹⁶ and PPN_2C_{60} ($0.086(5)\text{ \AA}$),⁴ and is close to that in the C_{60}^{2-} containing salts, $[M(NH_3)_6]C_{60} \cdot 6NH_3$, $M = Ni, Mn, \text{ and } Cd$ (0.0698 , 0.0648 , 0.0748 \AA ,⁵ respectively). Thus, C_{60}^{2-} has a moderate ellipsoidal deviation in **1**. It should be noted that the C_{60}^{2-} sphere is flattened along the *a*-axis.

The EPR spectrum of **1** at 290 K (room temperature, RT) has one broad single line with $g = 2.0006$ and the line half-width (ΔH) of 5.6 mT (signal I) overlapped with a very weak and narrow signal II (Figure 3). The total integral intensity of signal I reversibly increases with temperature in the 140 – 290 K range (Figure 3, inset). This allows the signal I to be attributed to the thermally populated excited triplet ($S = 1$) state of C_{60}^{2-} . The signal has unresolved low zero-field splitting ($D \cong 0$). This corresponds to a triplet state in which two unpaired electrons with parallel spins are sufficiently removed from each other that their interaction is not reflected in the EPR spectrum.^{7,9} The temperature decrease from 290 K down to 140 K results in both the shift of the *g*-factor to larger values and the essential narrowing of signal I ($g = 2.0016$ and $\Delta H = 0.5\text{ mT}$ at 140 K). The integral intensity of signal I at RT corresponds to $\sim 6\%$ population of the excited triplet state. The plot of $\ln(\text{integral intensity} \times T)$ versus $1/T$ is linear in the 290 – 140 K range (Figure 3, inset), and the slope of this plot affords the singlet–triplet energy gap of $730 \pm 10\text{ cm}^{-1}$ for C_{60}^{2-} in solid **1**.

(11) Picher, T.; Winkler, R.; Kuzmany, H. *Phys. Rev. B* **1994**, *49*, 15879.

(12) Robbins, J. L.; Edelstein, N.; Spencer, B.; Smart, J. C. *J. Am. Chem. Soc.* **1982**, *104*, 1882.

(13) Konarev, D. V.; Drichko, N.; Graja, A. *J. Chim. Phys.* **1998**, *95*, 2143.

(14) Boulas, P.; Jones, M. T.; Kadish, K. M.; Ruoff, R. S.; Lorents, D. C.; Malhotra, R.; Tse, D. S. *Proc. Electrochem. Soc.* **1994**, *94*–24, 1007.

(15) Crystallographic data for **1**: $C_{226}H_{138}Cl_4Co_4N_2$, $M_r = 3259.12$, black, monoclinic, space group $P2_1/m$, $a = 12.108(2)\text{ \AA}$, $b = 24.959(5)\text{ \AA}$, $c = 12.418(3)\text{ \AA}$, $\beta = 96.337(5)^\circ$, $V = 3729.8(13)\text{ \AA}^3$, $\rho_{\text{calcd}} = 1.451\text{ g}\cdot\text{cm}^{-3}$, $Z = 4$, $T = 120(2)\text{ K}$, data/restraints/parameters $11067/1812/1416$, final *R* indices [$I > 2\sigma(I)$], $R1 = 0.042$, $wR2 = 0.089$, $GOF = 1.015$.

(16) Wan, W. C.; Liu, X.; Sweeney, G. M.; Broderick, W. E. *J. Am. Chem. Soc.* **1995**, *117*, 9580.

(17) Bürgi, H.-B.; Blanc, E.; Schwarzenbach, D.; Liu, S.; Lu, Y.-J.; Kappes, M. M.; Ibers, J. A. *Angew. Chem., Int. Ed. Engl.* **1992**, *31*, 640.

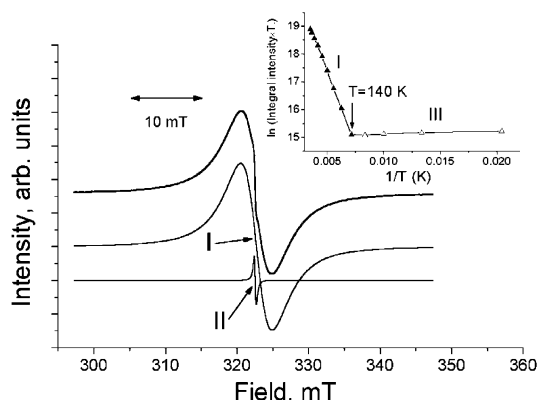


Figure 3. EPR signal of **1** at 290 K. The simulation of the signal by the two Lorentzian lines is shown below (broad signal I and narrow signal II). Inset shows the dependency of $\ln(\text{integral intensity} \times T)$ of the EPR signal I (290–140 K) and III (140–50 K) vs $1/T$ (see text).

Below 140 K (indicated by T in Figure 3, inset), signal I disappears, and only weak narrow signal III with the same g -factor is observed down to 4 K. The behavior of signal III in the 140–4 K range allows it to be distinguished from signal I. The intensity of signal III begins to increase as the temperature decreases. The plot of $\ln(\text{integral intensity} \times T)$ versus $1/T$ is nearly constant showing a paramagnetic dependency (Figure 3, inset). The g -factor shifts to smaller values ($g = 2.0009$ at 4 K), and ΔH remains constant (0.5 mT) down to 4 K. Moreover, this signal is superimposed on a weak signal with the splitting of 2.77 mT at $T < 100$ K. In the 140–4 K range, signal III cannot be attributed to the thermally populated excited triplet state of C_{60}^{2-} , and the integral intensity of this signal (about 0.3% of the total C_{60}) is too small for the ground state of C_{60}^{2-} . Probably the signal III originates from a small amount of the C_{60}^{2-} spins trapped on the defects.

The weak narrow signal II observed from 290 K down to 4 K (Figure 3) can be attributed to the reduction of the $C_{120}O$ impurity.¹⁰ Its integral intensity corresponds to 0.1% of total C_{60} , and the parameters ($g = 2.0008$, $\Delta H = 0.2$ mT at RT) are almost temperature independent.

The EPR behavior of **1** is similar to that of electrochemically generated C_{60}^{2-} in DMSO.⁹ Only a narrow line with $\Delta H = 0.2$ mT superimposed on the weak signal with splitting is observed at low temperatures (4.5–130 K). The intensity of these signals was calculated to be less than 4% of total C_{60} . The broad Lorentzian signal with $\Delta H = 3$ mT appears above 135 K. This signal was attributed to the thermally populated excited triplet state, which has about 6% occupation at 255 K. The singlet–triplet energy gap for C_{60}^{2-} in solution was determined to be 600 cm^{-1} .⁹ Only minor differences are seen for C_{60}^{2-} in solid **1**: (1) the contribution of the narrow EPR signal in the 4–140 K range is smaller (only 0.3% of the total C_{60}), (2) 6% occupancy of the triplet state is observed at higher temperature (290 K), and (3) the singlet–triplet energy gap is larger by 130 cm^{-1} .

SQUID measurements of solid **1** in the 1.9–300 K range are in agreement with the EPR data. The temperature dependency of molar magnetic susceptibility is presented in Figure 4. The sample holder contribution and the paramagnetic contribution of the Curie impurities (about 1%) were

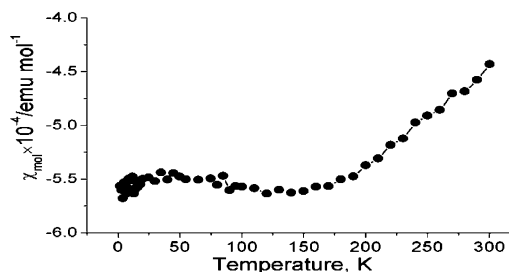


Figure 4. Temperature dependency of molar magnetic susceptibility (χ_{mol}) of **1** in the 1.9–300 K range.

subtracted from the experimental data. Susceptibility is negative and temperature independent in the 1.9–150 K range ($-5.6 \times 10^{-4} \text{ emu mol}^{-1}$). This value is close to the sum of core diamagnetic contributions from two Cp^*Co ($-4.6 \times 10^{-4} \text{ emu mol}^{-1}$)¹⁸ (Cp^*Co^+ has $S = 0^{12}$), C_{60} ($-2.52 \times 10^{-4} \text{ emu mol}^{-1}$),¹⁹ $C_6H_4Cl_2$ ($-0.83 \times 10^{-4} \text{ emu mol}^{-1}$), and C_6H_5CN ($-0.65 \times 10^{-4} \text{ emu mol}^{-1}$) moieties. Thus, **1** is diamagnetic in the 1.9–150 K range. Above 150 K, molar magnetic susceptibility increases because of the thermal population of the excited triplet state (Figure 4).

Thus, the EPR and SQUID data show that C_{60}^{2-} in solid **1** has a diamagnetic ground state ($S = 0$) at 2–140 K and only 6% population of the excited triplet state ($S = 1$) is observed at 290 K. The small amount of spins observed at low temperatures ($<0.4\%$ of total C_{60}) is most probably associated with defects or impurities. The similar low temperature narrow signals were observed for C_{60}^{2-} in solution⁹ and solid PPN_2C_{60} .⁷ The broad signal attributed to the triplet state ($T > 140$ K) was previously observed only in solution⁹ and was not found in solid PPN_2C_{60} .⁷ It is broad at RT and strongly narrows with the temperature decrease. The EPR signals from $C_{60}^{\bullet-}$ and $C_{60}^{\bullet 3-}$ radical anions ($S = 1/2$) behave similarly.³ However, in contrast to the signals from anion radicals, the integral intensity of the triplet signal in **1** decreases with temperature. The variable singlet–triplet energy gap for C_{60}^{2-} could be explained by the extent of the distortion from the I_h symmetry (due to the Jahn–Teller or crystal packing effects). Because of this, an ellipsoidal deviation for C_{60}^{2-} in PPN_2C_{60} larger than that in **1** can give a larger singlet–triplet energy gap. In this case, the population of the triplet state of C_{60}^{2-} in PPN_2C_{60} is rather small even at RT. Additional studies of the C_{60}^{2-} salts can allow the factors affecting the ellipsoidal deviation and the singlet–triplet energy gap for C_{60}^{2-} in the solid state to be elucidated.

Acknowledgment. The work was supported by the COE Research on Element Science 12CE2005, JSPS, and the RFBR Grant N03-03-32699.

Supporting Information Available: Additional experimental details and crystallographic data in CIF format. This material is available free of charge via the Internet at <http://pubs.acs.org>.

IC0340074

(18) Gebert, E.; Reis, A. H.; Miller, J. S.; Rommelmann, H.; Epstein, A. J. *J. Am. Chem. Soc.* **1982**, *104*, 4403. The core diamagnetic susceptibility for Cp^*Co must be close to that for Cp^*Fe since Fe^{2+} and Co^{2+} have close Pascal constants, -13 and $-12 \times 10^{-6} \text{ emu mol}^{-1}$, respectively.

(19) Ruoff, R. S.; Beach, D.; Cuomo, J.; McGuire, T.; Whetten, R. L.; Diederich, F. *J. Phys. Chem.* **1991**, *95*, 3457.